Rotary bistable and Parametrically Excited Vibration Energy Harvesting

L. Kurmann[1], **Y. Jia**[2], **D. Hoffmann**[3], **Y. Manoli**[3,4], **P. Woias**[5]

[1]University of Applied Sciences and Arts Northwestern Switzerland, School of Engineering, Inst. of Automation, Klosterzelgstrasse 2, 5210 Windisch, Switzerland
[2]University of Chester, Department of Mechanical Engineering, Thornton Science Park, University of Chester, Pool Lane, Chester CH2 4PU, United Kingdom
[3]Hahn-Schickard, W.-Schickard-Str. 10, 78052 Villingen-Schwenningen, Germany
[4]Fritz Huettinger Chair of Microelectronics, [5]Lab. for the Design of Microsystems, Department of Microsystems, Engineering – IMTEK, University of Freiburg, Georges-Köhler-Allee 102, 79110 Freiburg, Germany
E-mail: lukas.kurmann@fhnw.ch

Abstract. Parametric resonance is a type of nonlinear vibration phenomenon [1], [2] induced from the periodic modulation of at least one of the system parameters and has the potential to exhibit interesting higher order nonlinear behaviour [3]. Parametrically excited vibration energy harvesters have been previously shown to enhance both the power amplitude [4] and the frequency bandwidth [5] when compared to the conventional direct resonant approach. However, to practically activate the more profitable regions of parametric resonance, additional design mechanisms [6], [7] are required to overcome a critical initiation threshold amplitude. One route is to establish an autoparametric system where external direct excitation is internally coupled to parametric excitation [8]. For a coupled two degrees of freedom (DoF) oscillatory system, principal autoparametric resonance can be achieved when the natural frequency of the first DoF f_1 is twice that of the second DoF f_2 and the external excitation is in the vicinity of f_1. This paper looks at combining rotary and translatory motion and use autoparametric resonance phenomena.

1. Introduction

Energy Harvesting is a technology for capturing non-electrical energy from ambient energy sources, converting it into electrical energy and storing it to power wireless electronic devices. The process of capturing mechanical energy such as shocks and vibrations is a particular field of energy harvesting requiring specific types of energy harvesting devices, so called kinetic energy harvesters (KEH). There are many types of KEH's, but all of those systems have one common goal: an ideal KEH can keep the kinetic proof mass in resonance over an infinite large excitation bandwidth. Conventional, first generation types of such transducers can harvest mechanical vibration energy effectively only in a narrow frequency window. Over time many different types of systems have been analytically characterized, designed and tested. Most of these systems show only small improvements with respect to their bandwidth. None of those systems can transfer mechanical vibration power into electrical energy over a wide frequency band. The ideal kinetic harvester system will have a simple mechanical structure as well as a wide vibration frequency range for which the system can transfer effectively environmental mechanical vibrations into electrical energy. In this paper a new KEH system is analytically and numerically examined, assuming that the basepoint excitation source is infinite

(which for such small energies you can safely assume). In chapter 2.1. a mathematical system model is derived and in chapter 2.2. numerical simulations are presented.

2. Design of 2DoF bistable rotatory-translatory KEH

The lumped parameter model is depicted in Figure 1 having a rotary $\varphi(t)$ and a translatory $b(t)$ degree of freedom. The proof mass m_1 on cantilever l_1 with a 1st DoF $\varphi(t)$ can rotate on the pivot P_1 in the bounded region $\alpha_0 > |\varphi(t)|$, otherwise it will hit lobe N_1 or N_2 and might have hard or soft impact with a similar behavior treated in [3]. Perpendicularly attached ($\gamma_0 = 0°$) to l_1 at P_1 is a passive cantilever beam l_2. This cantilever has a translatory 2nd DoF $b(t)$ and carries an integrated piezoelectric (PE) transducer. On the tip of l_2 is a second proof mass m_2 carrying an electromagnetic (EM) transducer. The system is harmonically basepoint excited via y_0 and the mass m_1 at the end of cantilever l_1 is permanent-magnetically suspended (in a similar fashion as described in [9]) to introduce a linear k and nonlinear stiffness k_3 plus a translatory viscous damping d for the 1st DoF φ. The 2nd DoF b is similarly structured, having a linear stiffness k_b and a nonlinear stiffness k_{3b} (not depicted) plus a viscous damping d_b and an additional electromagnetic damping d_e. Depending on the angle γ_0, the cantilever length $l_{1,2}$ and the proof masses $m_{1,2}$, the system is in a monostable or bistable configuration. In case of the latter, the system has two stable energy wells, depicted in Figure 2, bottom diagram with $\varphi(t) = +\varphi_{01}$ and $b(t) = +b_{01}$. Its unstable equilibrium point is shaped by the mass ratio $\lambda_m = m_2 : m_1$ and given length ratio's $\lambda_l = l_2 : l_1$. In case both masses and lengths are equal, the unstable equilibrium position would be 45° (see also $\lambda_m = 1$ crossing the blue line ($\lambda_l = 1$) in top diagram of Figure 2).

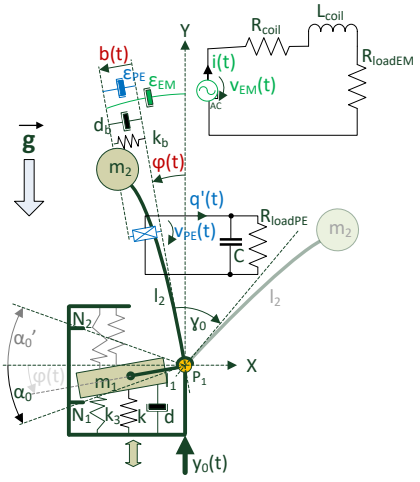

Figure 1. Lumped parameter model of the electromagnetic piezoelectric 2DoF KEH with 1. rotational DoF represented by $\varphi(t)$ and 2. translatory DoF represented by $b(t)$.

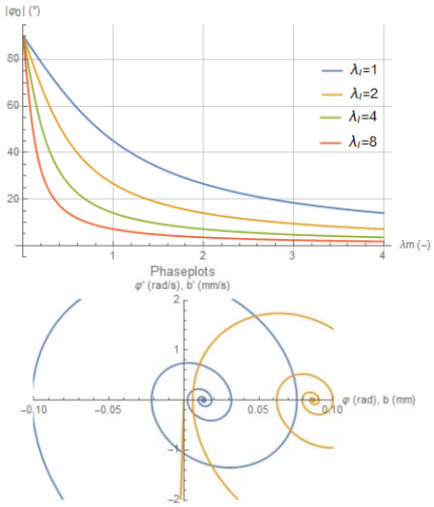

Figure 2. Initial position of φ_0 for the L-cantilever to achieve an unstable equilibrium (top) and the phase plots of $\varphi(t)$ and $b(t)$ with initial displacement and no excitation.

Cantilevers l_1, l_2 are assumed to have no mass and the quasi magnetically levitated mass m_1 on cantilever l_1 attached to the pivot P_1 transforms the translatory basepoint excitation y_0 into a rotary oscillation. The electromagnetic transducer damping (transduction factor ε_{EM} in [Vs/m]) is present in the mechanical domain in the resulting torque DE of $\varphi(t)$ and the force DE $b(t)$ whereas the piezoelectric damping (transduction factor ε_{PE} in [As/m]) is only present in the force DE $b(t)$. In this lumped parameter model the electrical circuit has an inductance L_{coil} and resistor R_{coil} and in series the resistive load R_{loadEM} attached. The piezoelectric transducer is drawn directly on the passive cantilever beam l_2 and the piezo-ceramic is modeled as capacitor C. It is a separately uncoupled circuit in the electrical domain with resistive load R_{loadPE}.

Figure 3 shows studies I-IV with different system angles γ_0. Several studies were conducted for achieving resonance over a large frequency range using following four principle parameters: (1) angle γ_0, (2) mass proportion factor λ_M, (3) proportionality of natural frequencies ω_1, ω_2 and (4) range of Ω

for analysis of sub-resonant and over-resonant response; in this paper only configuration I with system angle $\gamma_0 = 0°$ is presented.

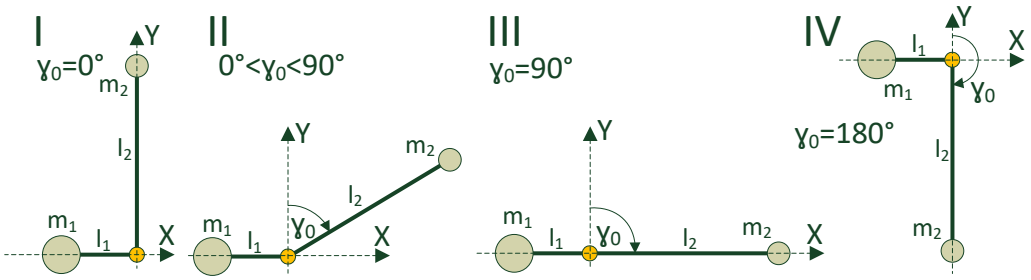

Figure 3. Configurations I-IV of the cantilever system; cantilever l_2 is a passive beam with stiffness k_b; in configuration I $\gamma_0 = 0°$, e.g. beams are perpendicular to each other.

2.1. Lumped parameter model of the 2DoF rotary-translatory KEH system

The equation of motion can be derived using the Lagrangian-Euler method, considering the system at first conservative. The Lagrangian total energy of this 2. DoF system is

$$L(\varphi, b) = T(\varphi, b) - V(\varphi, b) = 0 \tag{1}$$

The nonlinear magnetic spring shall be introduced directly via its energy (2).

$$F_S(y) = k\, y + k_3\, y^3 \;\rightarrow E_S = \int F_S(y)\, dy = \frac{1}{2} k\, y^2 + \frac{1}{4}\; k_3\, y^4 \tag{2}$$

Summing all kinetic T and potential V energies of this system and adding E_S of (2) to V yields

$$T(\varphi, b) = \frac{1}{2} m_2 \dot{b}^2 + \frac{1}{2} m_2 l_2 \cos\gamma_0\, \dot{b}\, \dot{\varphi} + \frac{1}{2} {l_1}^2 m_1 \dot{\varphi}^2 + \frac{1}{2} {l_2}^2 m_2 \dot{\varphi}^2 + \frac{1}{2} m_2 b^2 \dot{\varphi}^2 + l_2 m_2 \sin\gamma_0\, b\dot{\varphi}^2 \tag{3}$$

$$V(\varphi, b) = \frac{1}{2} k_b b^2 + \frac{1}{4} k_{3b} b^4 + g m_2 (l_2 \cos(\gamma_0 - \varphi) - b \sin\varphi) - g m_1 l_1 \sin\varphi + \frac{1}{2} k {l_1}^2 \sin^2\varphi + \frac{1}{4} k_3 {l_1}^4 \sin^4\varphi \tag{4}$$

In (4) also a nonlinear spring for the cantilever beam is introduced in the same fashion as the magnetic spring using linear beam stiffness k_b and nonlinear stiffness k_{3b}. Following the Lagrangian formalisms and writing the set of DE dimensionless using ω_1 as reference will lead to following set:

$$\begin{gathered}\theta''\left(1 - \lambda_m + \lambda_m\, {\lambda_l}^2 - 2\lambda_l \lambda_m \sin\gamma_0\, u + \lambda_m u^2\right) + 2\xi_1 \sin\theta\, \theta' + \cos\theta \sin\theta\, (1 + \beta \sin^2\theta\,) + 2\lambda_m u u' \theta' \\ + \varrho \cos\theta\, (-1 + \lambda_m - \lambda_m u) + \varrho \lambda_l \lambda_m \sin(\gamma_0 - \theta) - 2\lambda_l \lambda_m \sin\gamma_0\, u'\theta' + \lambda_l \lambda_m \cos\gamma_0\, u'' + \kappa_E \zeta = -\lambda\, \Omega^2 \cos(\Omega\tau) \sin\theta\end{gathered} \tag{5}$$

$$u'' + 2\xi_2\, \Omega_0\, u' + {\Omega_0}^2\, u(1 + \beta_b u^2) + \lambda_l \cos\gamma_0\, \theta'' - u{\theta'}^2 + \lambda_l \sin\gamma_0\, {\theta'}^2 - \varrho \sin\theta + \kappa_E \lambda_l {\lambda_m}^{-1}\, \zeta + \kappa_P \lambda_P \lambda_l\, {\Omega_0}^2 \upsilon = 0 \tag{6}$$

$$\lambda_E\, {\lambda_l}^{-1} \Omega_0\, u' + \lambda_E\, \theta' = \zeta' + \lambda_E\, \zeta \tag{7}$$

$$u + \lambda_P \upsilon = \rho \tag{8}$$

$$\rho' = -\upsilon \tag{9}$$

Using following parameters for nondimensionalization (using ω_1 as reference):

$$\lambda = \frac{A}{l_1};\; \lambda_l = \frac{l_2}{l_1};\; \lambda_M = \frac{m_2}{m_1 + m_2} = \frac{m_2}{m};\; \Omega = \frac{\omega}{\omega_1};\; \tau = t\omega_1;\; \xi_1 = \frac{d}{2m_1\omega_1}; \xi_2 = \frac{d_b}{2m_2\omega_2} \tag{10a}$$

$${\omega_1}^2 = \frac{k}{m_1 + m_2}\;; {\omega_2}^2 = \frac{k_b}{m_2};\;\; {\Omega_0}^2 = \frac{{\omega_2}^2}{{\omega_1}^2};\; \varrho = \frac{g}{l_1 {\omega_1}^2}; \beta = \frac{k_3}{k}\, {l_1}^2; \beta_b = \frac{k_{3b}}{k_b}\, {l_1}^2 \tag{10b}$$

$$i_{e0} = \frac{\varepsilon_{EM}\, l_2\, \omega_1}{R}; v_{p0} = R\, \omega_2 q_{p0};\; q_{p0} = \varepsilon_{PE}\, l_2;\; \kappa_E = \frac{\varepsilon_{EM}{}^2}{m\, R\, \omega_1};\; \kappa_P = \frac{\varepsilon_{PE}{}^2}{C\, k_b}; \lambda_E = \frac{R}{L\, \omega_1}; \lambda_P = RC\omega_2 \tag{10c}$$

$$\text{angle}\; \theta(\tau) = \frac{\varphi(t)}{\varphi_0},\; \text{path}\; u(\tau) = \frac{b(t)}{l_1},\; \text{EM current}\; \zeta(\tau) = \frac{i_e(t)}{i_{e0}},\; \text{PE voltage}\; \upsilon(\tau) = \frac{v_p(t)}{v_{p0}},\; \text{charge}\; \rho(\tau) = \frac{q_p(t)}{q_{p0}} \tag{10d}$$

Note also that above set of equation is highly nonlinear and not reflected in above set of DE is the impact when θ reaches $\pm\alpha_0$; see also [3] for a possible nomenclature of such conditions.

2.2. Mechanical domain (θ and u) and electrical domain (ζ, υ, ρ) response

Extensive dimensioned and dimensionless simulations were conducted with Mathematica and Matlab Simulink (solvers ODE23 of Bogacki-Shampine and ODE45 of Dormand-Price) using the coupled DE system (5)-(9) and corresponding parameters for nondimensionalization (10a)-(10d) to investigate the dynamics of this highly nonlinear system. In the following simulations an impact of m_1 into the supporter structure at $N_{1,2}$ (shown in Figure 1) will result in a light elastic impact and its impact velocity is reversed to 40% of its impact velocity.

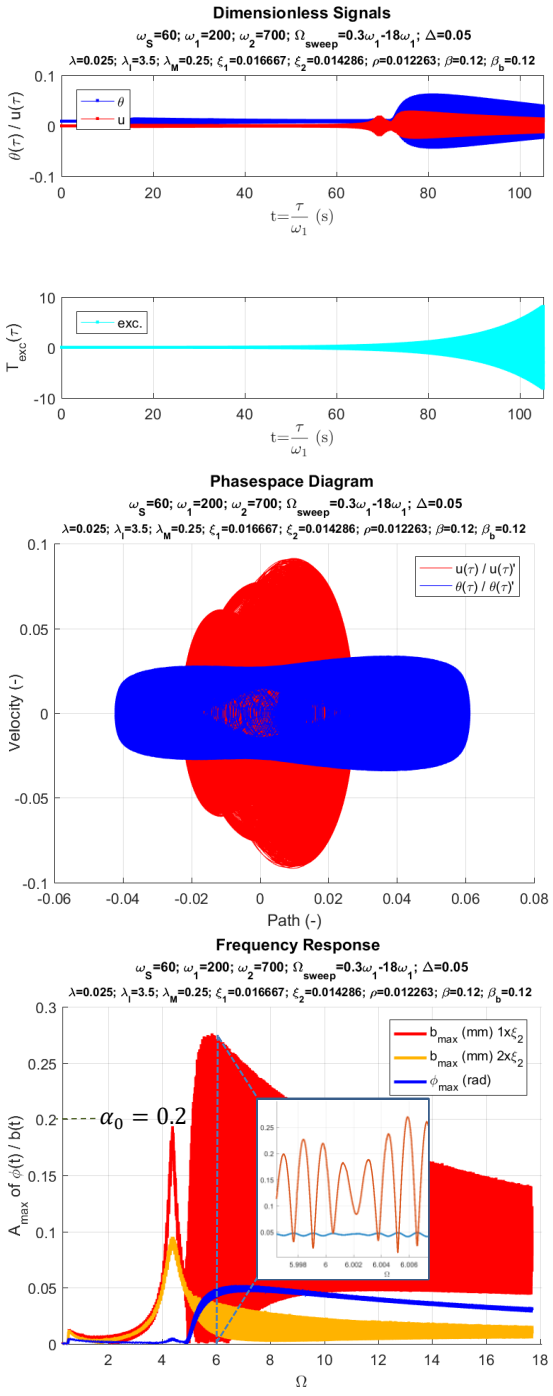

Figure 4. Dimensionless response and input (top); phase space behavior on upward sweep (middle) and its corresponding frequency-response (bottom)

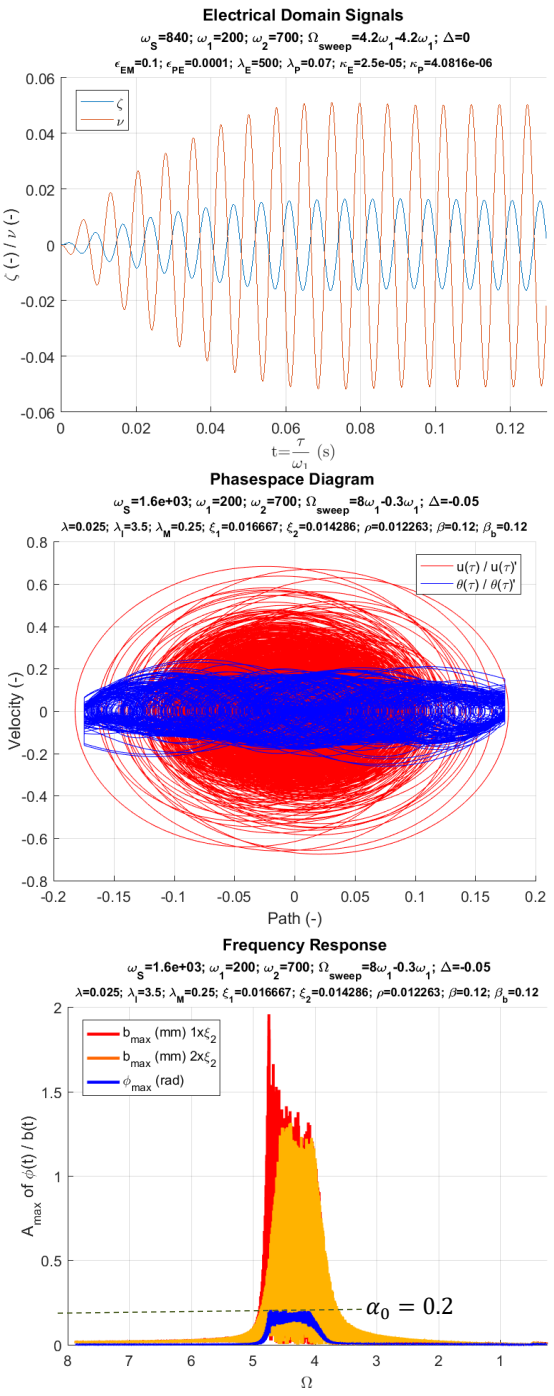

Figure 5. Dim. less response of PE voltage and EM current (top); phase space behavior of downward sweep and its corresponding frequency-response (bottom)

Particular attention was given to the initial positions of the system θ, θ' and u, u', as depending on its configuration, an initial torque is created, which puts the system not in rest. For example, if the starting condition of θ will be set to α_0 using also an according weak stiffness – the angle θ might stay at the oscillating lobe N_1 (depending heavily also of all system parameters) and the 2nd DoF u will show in such a case only a classic linear frequency response. For having a broadband response, m_1 needs to be able to exert a slight oscillation (for configuration I with $\lambda_M = 0.25$).

Figure 4 depicts mechanical domain diagrams, top and middle diagrams show responses dimensionless, bottom diagram depicts the frequency response of $\varphi \equiv \phi$ and $u \equiv b$. Top and middle diagram of Figure 5 show dimensionless electrical response and phase space response, bottom diagram depicts the frequency response of ϕ and b. Top diagram of Figure 4 shows excitation signal of an upward frequency sweep ($\Omega = 0.3 - 18$) in light blue; for each frequency step-cycle 40 periods are used and an amplitude step of $\Delta = 0.05\Omega$ is applied. The system in this configuration is set to have its natural frequencies at $\omega_1 : \omega_2 = 1 : 3.5$ (like its λ_l relation; other frequency ratios were tested, $\omega_1 : \omega_2 = 1 : 3$ exerts similar results, but not $\omega_1 : \omega_2 = 1 : 2$). The damping of θ and u is set to $d = 0.1Ns/m$; in case both damping factors are doubled, resulting amplitudes are at least reduced by factor 6 with exception of the subharmonic response at $\Omega = 0.5$ on an upward seep (depicted in orange, bottom diagram in Figure 4). On a downward sweep, the amplitudes are only reduced by ca. 20% (depicted in orange, bottom diagram in Figure 5). The excitation amplitude is set to $A = 0.5mm$. If a smaller amplitude is used, the system will not behave as depicted in Figure 4 and Figure 5. The response of b and ϕ, particularly ϕ is showing a beat frequency. In the electrical domain, the advantage of having a PE and EM transducer coupled is the resulting 180° phase shift of current and voltage (see also Figure 5, top diagram) which is particularly useful for a DC-DC converter next in line.

3. Conclusions

Presented KEH system is a new approach for the realization of a wideband KEH. Such a device can also be tuned to different environmental frequency bands by simply setting the system cantilever angle γ_0 (see Figure 3). This KEH system is discussed only for bi-stable configuration I, but additional bi-stable (II) and mono-stable (III and IV) configurations are available. It shows a particularly large and long resonance on an upward sweep ($\Omega = 5 - 18$), above the detuned system resonance of $\Omega \approx 4.4$ (which is always accessible, e.g. independent of the frequency sweep direction). Like in all nonlinear systems, the hysteresis causes to access this large frequency band only by tuning into this region with an upward frequency sweep. Having a downward frequency sweep (Figure 5, middle and bottom), also a resonance region is found with ca. 6x larger amplitudes for b and ca. 3.5x larger for φ resulting in an impact behavior where φ reaches α_0 (Figure 5, bottom/middle) in the region of $\Omega = 5 - 3.8$.

References

[1] N. Minorsky, „Nonlinear Oscillations“, Princeton, N.J., Van Nostrand, 1962

[2] A. Nayfeh, D. Mook, „Nonlinear Oscillation“, Weinheim, Wiley, 2007

[3] L. Kurmann, D. Hoffmann, B. Folkmer, Y. Manoli, P. Woias, R. Anderegg, “Autoparametric resonance systems for vibration-based energy harvesters”, J. Phys. Conf. Ser., vol. 660, p. 012070, 2015

[4] Y. Jia, J. Yan, K. Soga, and A. Seshia, “A parametrically excited vibration energy harvester”, J. Intel. Mat. Syst. Str., 2013.

[5] Y. Jia, J. Yan, K. Soga and A. A. Seshia, “Multi-frequency operation of a mems vibration energy harvester by accessing five orders of parametric resonance”, in J. Phys. Conf. Ser., ser. 1, vol. 476, 2013, pp. pp. 607–611

[6] Y. Jia, J. Yan, K. Soga, and A. A. Seshia, “Parametric resonance for vibration energy harvesting with design techniques to passively reduce the initiation threshold amplitude”, Smart Mater. Struct., vol. 23, no. 6, p. 13, 2014.

[7] Y. Jia, J. Yan, K. Soga, and A. Seshia, “Parametrically excited mems vibration energy harvesters with design approaches to overcome initiation threshold amplitude”, J. Micromech. Microeng., vol. 23, no. 11, p. 10pp., 2013.

[8] Y. Jia and A. A. Seshia, “An auto-parametrically excited vibration energy harvester”, Sens. Actuators A, vol. 220, pp. 69–75, 2014.

[9] B. P. Mann, N. D. Sims, “Energy harvesting from the nonlinear oscillations of magnetic levitation”, J. Sounds and Vibration, 319, pp. 515–530, 2009.